



Size distribution and clothing-air partitioning of polycyclic aromatic hydrocarbons generated by barbecue

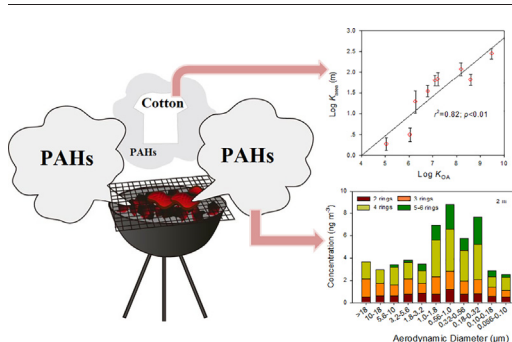
Jia-Yong Lao, Chen-Chou Wu, Lian-Jun Bao, Liang-Ying Liu, Lei Shi, Eddy Y. Zeng*

School of Environment, Guangdong Key Laboratory of Environmental Pollution and Health, Jinan University, Guangzhou 511443, China

HIGHLIGHTS

- Particle-bound PAHs derived from BBQ fumes were affiliated with fine particles.
- Particulate PAHs in BBQ fumes were from by combustion of charcoal, fat in food, and oil.
- Log $K_{\text{clothing-air}}$ and log K_{oa} of PAHs were significantly correlated with each other.

GRAPHICAL ABSTRACT



ARTICLE INFO

Article history:

Received 8 April 2018

Received in revised form 17 May 2018

Accepted 18 May 2018

Available online xxx

Editor: Kevin V. Thomas

Keywords:

Polycyclic aromatic hydrocarbons

Barbecue fumes

Size-dependent distribution

Source diagnostics

Clothing-air partitioning

ABSTRACT

Barbecue (BBQ) is one of the most popular cooking activities with charcoal worldwide and produces abundant polycyclic aromatic hydrocarbons (PAHs) and particulate matter. Size distribution and clothing-air partitioning of particle-bound PAHs are significant for assessing potential health hazards to humans due to exposure to BBQ fumes, but have not been examined adequately. To address this issue, particle and gaseous samples were collected at 2-m and 10-m distances from a cluster of four BBQ stoves. Personal samplers and cotton clothes were carried by volunteers sitting near the BBQ stoves. Particle-bound PAHs (especially 4–6 rings) derived from BBQ fumes were mostly affiliated with fine particles in the size range of 0.18–1.8 μm. High molecular-weight PAHs were mostly unimodal peaking in fine particles and consequently had small geometric mean diameters and standard deviations. Source diagnostics indicated that particle-bound PAHs in BBQ fumes were generated primarily by combustion of charcoal, fat content in food, and oil. The influences of BBQ fumes on the occurrence of particle-bound PAHs decreased with increasing distance from BBQ stoves, due to increased impacts of ambient sources, especially by petrogenic sources and to a lesser extent by wind speed and direction. Octanol-air and clothing-air partition coefficients of PAHs obtained from personal air samples were significantly correlated to each other. High molecular-weight PAHs had higher area-normalized clothing-air partition coefficients in cotton clothes, i.e., cotton fabrics may be a significant reservoir of higher molecular-weight PAHs.

Capsule: Particle-bound PAHs from barbecue fumes are generated largely from charcoal combustion and food-charred emissions and mainly affiliated with fine particles.

© 2018 Elsevier B.V. All rights reserved.

1. Introduction

Cooking fumes contain a large number of organic contaminants, such as polycyclic aromatic hydrocarbons (PAHs), which vary from

* Corresponding author.

E-mail address: eddyzeng@jnu.edu.cn (E.Y. Zeng).

different cooking styles and cooking oils, among others (Amouei Torkmahalleh et al., 2017; Gao et al., 2015; Wang et al., 2015; Yao et al., 2015). Compared to other cooking methods, barbecue (BBQ) was reported to emit the highest levels of PAHs and suspended particulates (Chen et al., 2012; Wang et al., 2017; Yao et al., 2015). Although BBQ may be one of the most popular outdoor and indoor cooking events around the world, BBQ fumes have not yet been investigated adequately. Wu et al. (2015) found that the maximum potential health risk via dermal and inhalation exposure to BBQ fumes for 1 h per day was 1.4×10^{-4} , slightly higher than the upper limit of the incremental lifetime cancer risk range (1×10^{-6} – 1×10^{-4}) (USEPA, 2017). Badyda et al. (2018) also suggested that inhalation exposure risk to BBQ particles for 5 h a day and 40 days a year was as high as 8.68×10^{-1} . Many previous findings indicated that PAHs were strongly size-dependent, which would influence the deposition of PAHs in different regions of the human respiratory tract (Burkart et al., 2013; Luo et al., 2015; Schnelle-Kreis et al., 1999; Wu et al., 2015). As a result, formation and characteristics of particle-bound PAHs derived from BBQ merit further investigations.

Polycyclic aromatic hydrocarbons in BBQ fumes are generated by incomplete burning and pyrolysis of thermal agents, food nutrients, and food oil and fat contents (Farhadian et al., 2011; Oz and Yuzeer, 2016; Rey-Salgueiro et al., 2008). Therefore, the types of fuel and food dictate the formation of PAHs. Charcoal, natural and liquefied gas, and electricity are often used in BBQ, and charcoal is preferable, especially for Europeans, as it can generate high temperature and smoke leading to tasteful cooked meat (Mode, 2017). The type of fuels was reported to influence the formation of particle-bound PAHs in BBQ fumes, with charcoal briquettes producing the largest amount of PAHs (Badyda et al., 2018). Abundance and size distribution of PAHs emitted from BBQ are also impacted by food ingredients and oil, particularly by fat-rich food, but carbohydrates and proteins of food are not involved in the formation of PAHs (Saito et al., 2014). Knowledge gap has remained about the primary and other potential sources of particle-bound PAHs in BBQ fumes and how PAHs evolve upon being emitted.

Dermal contact is an important route for human exposure to PAHs. Clean clothes may be able to protect human skins from sorption of semi-volatile organic compounds, whereas clothes pre-exposed to these pollutants can enhance dermal uptake (Morrison et al., 2015c). Accumulation of cooking fume derived PAHs on clothes is therefore significant for human health and should be well characterized. Most previous studies have focused on clothing-air partition coefficients of nicotine, phthalates, polybrominated diphenyl ethers (PBDEs), polychlorinated biphenyls (PCBs), and halogenated flame retardants, but not PAHs, possibly because of low PAH concentrations in offices or homes (Li et al., 2010; Morrison et al., 2018; Morrison et al., 2015a; Saini et al., 2017; Saini et al., 2016). To address this issue, cotton clothes were chosen to conduct exposure experiments during outdoor BBQ events using charcoal. Particulate samples collected in 11 size fractions were analyzed for 16 PAHs, from which size-dependent concentration data were acquired to assess the formation and potential sources of PAHs. The clothing-air partition coefficients of PAHs derived from BBQ fumes were also estimated.

2. Materials and methods

2.1. Materials

A standard solution containing 16 priority PAHs was purchased from AccuStandard (New Haven, CT, USA), i.e., naphthalene (Nap), acenaphthylene (Acy), acenaphthene (Ace), fluorene (Flu), phenanthrene (Phe), anthracene (Ant), fluoranthene (Fla), pyrene (Pyr), benzo[*a*]anthracene (BaA), chrysene (Chr), benzo[*b*]fluoranthene (BbF), benzo[*k*]fluoranthene (BkF), benzo[*a*]pyrene (BaP), indeno[1,2,3-*cd*]pyrene (IcdP), dibenz[*a,h*]anthracene (DahA), and benzo[*ghi*]perylene (BghiP). The sum of BbF and BkF is designated as B[b + k]F. Surrogate standards

and internal standards were described previously (Wu et al., 2015). XAD resins were obtained from Supelco (Bellefonte, PA, USA).

2.2. Sample collection

Barbecuing was conducted on November 5, 2016 in suburban Guangzhou. Particle samples were collected on 47-mm diameter glass microfibre filters (Whatman International, Maidstone, England) with Micro-Orifice Uniform Deposit Impactor (MOUDI; MSP Corporation, Shoreview, MN, USA), and segregated into 11 size fractions: >18, 10–18, 5.6–10, 3.2–5.6, 1.8–3.2, 1.0–1.8, 0.56–1.0, 0.32–0.56, 0.18–0.32, 0.10–0.18, and 0.056–0.10 μm . Gaseous samples were collected in polyurethane foam (PUF) at the end of the MOUDI sampler with a constant flow rate of 30 L min^{-1} . Sampling sites were selected at 2 and 10 m away from four barbecue stoves arranged as a rectangle (Supplementary data Fig. S1; “S” designates texts, tables, and figures in the Supplementary data), and 1.2 m above the ground. Each personal air sampler equipped with 1.65 g of mixed XAD-2 and XAD-4 resin (1:1 in mass) and an active sampling device at a flow rate of 3 L min^{-1} was operated by volunteers to collect personal air samples, which were assumed to be 0 m away from the BBQ stoves. The time duration of sampling by both MOUDI and personal samplers was 2.5 h. Related cotton clothing samples were also collected by volunteers. In total, two particle samples (each contained 11 sub-samples of different size ranges), two gaseous samples, 13 personal air samples, 13 clothing samples, and four field blank samples were collected and stored in $-20\text{ }^{\circ}\text{C}$ until analysis.

2.3. Sample extraction and instrumental analysis

All samples were spiked with the surrogate standards before extraction, and the procedures for extraction and purification of gaseous, particle, and clothing samples were described previously (Wu et al., 2015). Each personal air sample collected with XAD was ultrasonically extracted three times, each with 15 mL mixture of hexane, dichloromethane, and acetone (2:2:1 in volume). The combined extract was dried with anhydrous sodium sulfate and purified on a neutral silica gel column with hexane as the eluent. The collected extract was further concentrated to 50 μL in a vial under a gentle stream of N_2 and spiked with the internal standards before instrumental analysis.

Measurements of PAHs were performed by a Shimadzu GCMS-2010 Plus in the electron impact mode, with chromatographic separation by a DB-5MS capillary column (30 m \times 0.25 mm i.d. with 0.25 μm film thickness). The column oven temperature was programmed from 60 $^{\circ}\text{C}$ (held for 1 min), increased to 200 $^{\circ}\text{C}$ at a rate of 20 $^{\circ}\text{C min}^{-1}$ (held for 3 min), raised to 250 $^{\circ}\text{C}$ at 15 $^{\circ}\text{C min}^{-1}$ (held for 4 min), and finally increased to 300 $^{\circ}\text{C}$ at 25 $^{\circ}\text{C min}^{-1}$ (held for 12 min). The ion source temperature was set at 250 $^{\circ}\text{C}$ and full scanning from m/z 35 to m/z 350 was conducted.

2.4. Quality assurance and quality control

The recoveries of the surrogate standards, i.e., naphthalene- d_8 , acenaphthene- d_{10} , phenanthrene- d_{10} , chrysene- d_{12} , perylene- d_{12} , and benzo[*ghi*]perylene- d_{12} , were $54 \pm 10\%$, $66 \pm 13\%$, $82 \pm 19\%$, $94 \pm 21\%$, $86 \pm 20\%$, and $84 \pm 16\%$ in field samples, and $68 \pm 17\%$, $73 \pm 11\%$, $81 \pm 10\%$, $98 \pm 13\%$, $90 \pm 13\%$, and $89 \pm 6\%$ in blank samples. Concentrations of PAHs in field samples were corrected by those in corresponding procedural blanks within the same batch. The lowest calibration concentrations divided by the actual sample volumes/areas were defined as the reporting limits. The reporting limit was 0.056 ng m^{-3} with an air volume of 4.5 m^3 for gaseous and particle samples, 0.56 ng m^{-3} with an air volume of 0.45 m^3 for personal air samples, and 12.5 ng m^{-2} with a fabric area of 0.04 m^2 for clothing samples.

2.5. Data analysis

The area normalized fabric-air partition coefficient (K_{area}) was estimated by (Morrison et al., 2018)

$$K_{\text{area}} = \frac{m_{\text{PAH}}}{A_{\text{sample}} C_{\text{PAH}}} \quad (1)$$

where m_{PAH} is the mass of a PAH compound extracted from cotton cloth sample; A_{sample} is the clothing surface area; and C_{PAH} is the gaseous concentration of the PAH compound. Geometric mean diameter (GMD) and geometric standard deviation (GSD) were calculated by (Luo et al., 2015)

$$\log \text{GMD} = \frac{\sum (C_i \times \log D_{p,i})}{\sum C_i} \quad (2)$$

$$(\log \text{GSD})^2 = \frac{\sum [C_i \times (\log D_{p,i} - \log \text{GMD})^2]}{\sum C_i} \quad (3)$$

where C_i and $D_{p,i}$ are the target concentration and geometric mean particle sizes (Bi et al., 2005; Bi et al., 2003). High molecular-weight PAHs (5–6 rings), except for B[b + k]F, showed unimodal size distribution patterns peaking in the fine particle fraction (Fig. 2), probably because they tend to affiliate with fine particles due to their high octanol-air partition coefficients (Odabasi et al., 2015). The characteristic times for re-partitioning of high molecular-weight PAHs, with lower vapor pressures, are also much longer than those for low molecular-weight PAHs (Bi et al., 2005).

3. Results and discussion

3.1. Characteristic of particle-bound PAHs size distribution

Among the target PAHs measured in BBQ fumes, DahA was not detected in samples collected from both the 2-m and 10-m sites from the BBQ stoves. Concentrations of PAHs in ambient air were higher at 2-m than at 10-m from the stoves (Fig. S2), apparently due to the impacts from the BBQ stoves. This variability in PAH concentrations with distance from emission sources was not only consistent with the results for BBQ fumes in Urumqi, China (Wu et al., 2015), but also with those for traffic sources (Lee et al., 1995). Fewer high molecular-weight PAHs were detected at the 10-m site, especially for IcdP and BghiP, than low molecular-weight ones (Fig. S2). This may have been caused by atmospheric turbulence and dilution effects due to high wind speed (Burkart et al., 2013).

Previous studies demonstrated that the distribution of PAHs was particle size-dependent and predominantly associated with fine particles (Aceves and Grilmalt, 1993; Burkart et al., 2013; Luo et al., 2015; Odabasi et al., 2015; Schnelle-Kreis et al., 1999). In the present study, particle-bound PAHs, especially 4–6 ring PAHs, were dominant in the size range of 0.18–1.8 μm (Fig. 1), defined as the accumulation mode. The prevailing occurrence of PAHs in fine particles from BBQ fumes was likely resulted from primary combustion emissions and coagulation

and/or condensation of gaseous PAHs on pre-existing particle surfaces (Bi et al., 2005). In addition, ultrafine particles ($<0.1 \mu\text{m}$) contained considerable amounts of 5–6 ring PAHs at the 2-m site (Fig. 1). As ultrafine particles possess large surface areas and great ability to sorb and condense toxic air pollutants, they present severe threats to human health (Sioutas et al., 2005). In this context, inhalation exposure to BBQ fumes merits further examination.

At the 2-m site, low molecular-weight PAHs (Ace, Flu, and Phe) were slightly unimodal in size distribution with a peak in fine particles ($<1 \mu\text{m}$), and well distributed in ultrafine and coarse particles (Fig. 2). However, Ant, Fla, and Pyr showed somewhat bimodal distribution patterns (Fig. 2), contrary to the results from our previous study in Urumqi (Wu et al., 2015), where the size distributions of PAHs were all unimodal at the 2-m site away from a BBQ stove. The difference may have been attributed to the higher concentrations of low molecular-weight PAHs in the gaseous phase than in the particulate phase (both normalized to ng m^{-3}) in the present study (Fig. S2), resulting in easier gas-to-particle condensation on pre-existing particles (dust, soil or particles from combustion sources). This allowed low molecular-weight PAHs to more easily maintain equilibrium between particles of different sizes.

At the 10-m site, particle-bound PAHs were generally unimodal size distributed and low molecular-weight PAHs (Flu, Phe, Ant, Fla, and Pyr) tended to shift from coarse particles to fine particles (Fig. 3), opposite to previously reported results that long-distance transport would shift particle-bound chemicals from fine to large size fractions (Bi et al., 2005; Kavouras and Stephanou, 2002; Van Vaeck and Van Cauwenberghe, 1985). It is possible that coarse particles have higher dry deposition velocity than fine particles (Luo et al., 2015); consequently they may deposit faster during transport. Other emission sources and/or meteorological conditions (e.g., wind direction and speed and temperature) would also strongly affect the size distribution of PAHs, e.g., shifting toward larger particles (Schnelle-Kreis et al., 1999).

The GMD values of individual particle-bound PAHs were in the ranges of 0.43–3.27 and 0.60–1.56 μm at the 2-m and 10-m sites, respectively, with GSDs being 1.93–5.81 and 1.00–5.12 μm (Table 1). Previous studies indicated that particle-bound PAHs had smaller GMDs with shorter distances to emission sources (Schnelle-Kreis et al., 1999; Wu et al., 2015). In the present study, however, the GMDs of 2–4 ring

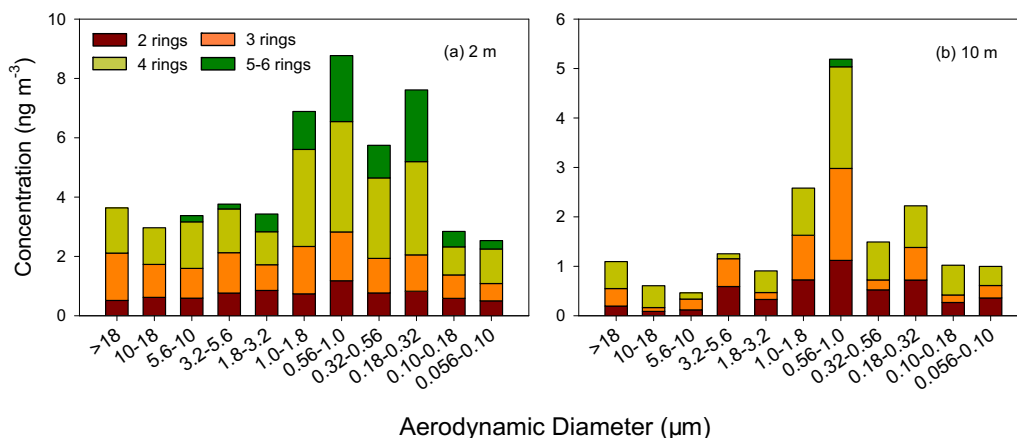


Fig. 1. Concentrations (ng m^{-3}) of particle-bound PAHs in 11 size fractions at (a) 2-m and (b) 10-m sites near BBQ stoves.

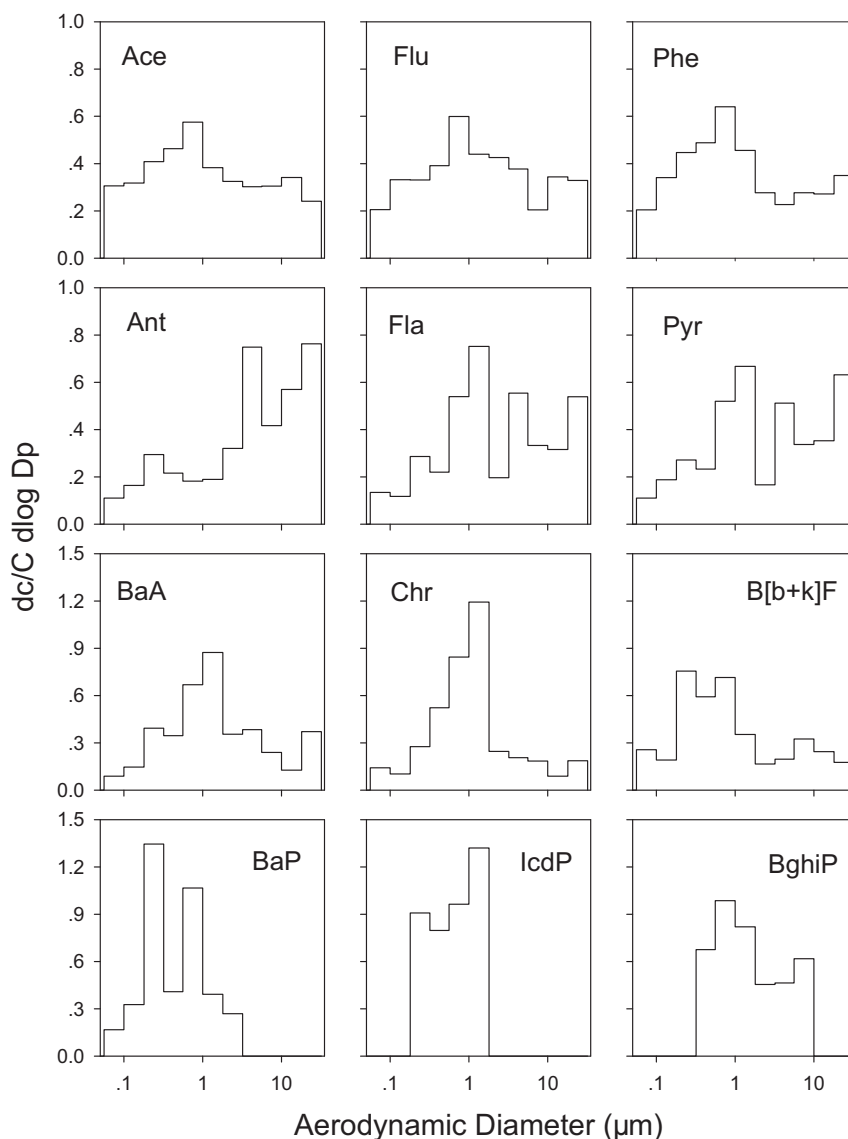


Fig. 2. Particle size distributions of PAHs at 2 m from BBQ stoves, where dc is the mass concentration of PAHs in each size fraction, C is the total mass concentration of particle-bound PAHs, and $d\log D_p$ is the logarithm of aerodynamic diameter size interval between two adjacent size fractions.

PAHs were greater at the 2-m site than at the 10-m site, probably due to higher concentrations of 2–4 ring PAHs in the gaseous phase which facilitated redistributing toward pre-existing coarse particles by volatilization and condensation. Gas-to-particle condensation of PAHs on pre-existing larger particles upon emitting from sources such as charcoal ash, suspended dust, and soil may have also contributed to the particle size variability. Meteorological conditions (e.g., relative humidity) are another significant factor controlling the particle size distribution (Burkart et al., 2013; Tsapakis and Stephanou, 2005). For example, high relative humidity may enhance the sorption of PAHs with high octanol-water coefficients on particles (Burkart et al., 2013). Because sampling was conducted on a river bank in the present study, its relative humidity was higher than that of Urumqi in August, resulting in wider size ranges of particle-bound PAHs with higher GMD values. However, the results of high molecular-weight PAHs with lower GMDs and GSDs in the present study (Table 1) were consistent with those acquired in Guangzhou and Urumqi (Luo et al., 2015; Wu et al., 2015). The GSD values are generally larger for chemicals with higher vapor pressures than those with lower ones due to the effects of volatilization (Luo et al., 2015).

3.2. Diagnostics of potential PAH sources

The ratios of PAH isomers with similar physicochemical properties, such as $Fla/(Fla + Pyr)$, $Ant/(Ant + Phe)$, $BaA/(BaA + Chr)$, and $IcdP/(IcdP + BghiP)$, have been suggested as indicators of pyrogenic or petrogenic sources (Dvorská et al., 2011; Katsoyiannis et al., 2011; Wang et al., 2016; Yunker et al., 2002). In general, $Fla/(Fla + Pyr) > 0.4$, $Ant/(Ant + Phe) > 0.1$, and $BaA/(BaA + Chr) > 0.35$ indicate pyrogenic emissions, while $Fla/(Fla + Pyr) < 0.4$, $Ant/(Ant + Phe) < 0.1$, and $BaA/(BaA + Chr) < 0.2$ suggest petrogenic origins (Budzinski et al., 1997; Dvorská et al., 2011; Katsoyiannis et al., 2011; Yunker et al., 2002). It should be noted that use of PAH isomeric ratios without robust source and transport information to diagnose potential input source may incur large uncertainties. The conclusions drawn below should be considered as being supplementary to the main findings.

At the 2-m site, $Fla/(Fla + Pyr)$ and $Ant/(Ant + Phe)$ in all particle size ranges were >0.4 and >0.1 , respectively, whereas $BaA/(BaA + Chr)$ was >0.35 in most particle size ranges (Table 2), suggesting dominant pyrogenic emissions (Budzinski et al., 1997; Katsoyiannis et al., 2011; Yunker et al., 2002). Furthermore, the $Fla/(Fla + Pyr)$ values

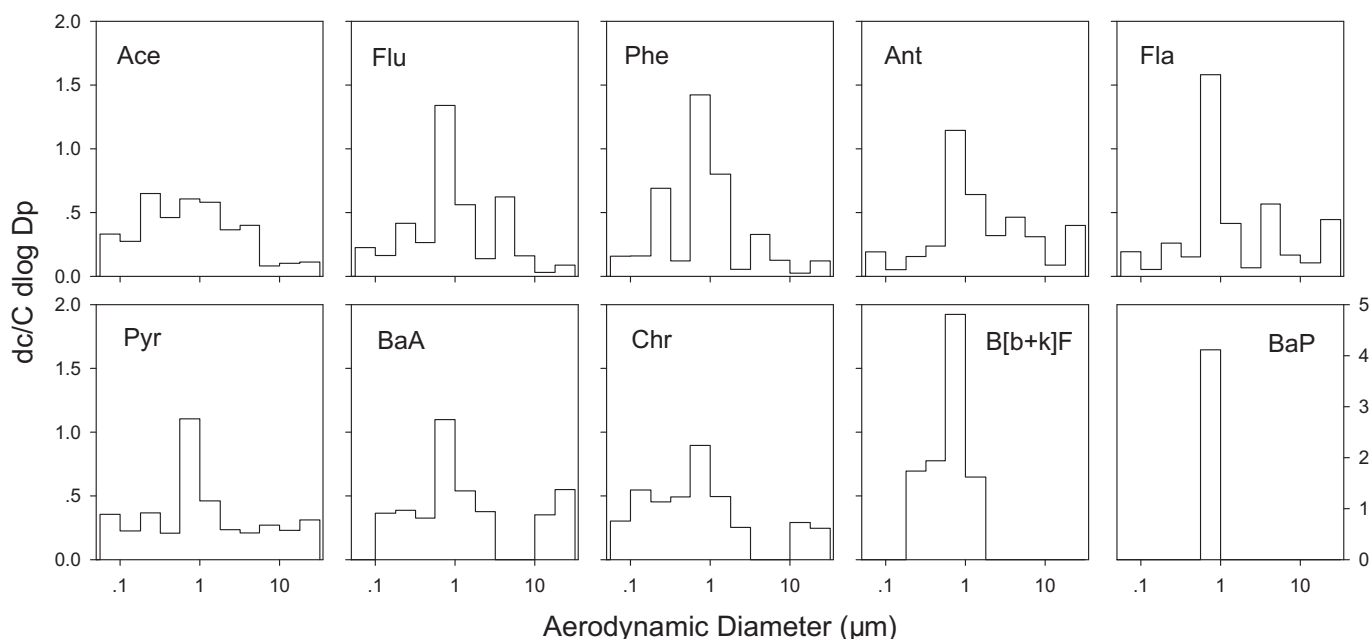


Fig. 3. Particle size distributions of PAHs at 10-m from BBQ stoves, where d_c is the mass concentration of PAHs in each size fraction, C is the total mass concentration of particle-bound PAHs, and $d \log D_p$ is the logarithm of aerodynamic diameter size interval between two adjacent size fractions.

in most size ranges were >0.5 (Table 2), indicating a predominant influence by combustion of wood or charcoal instead of fuel burning (Katsoyiannis et al., 2011). Average values of Fla/(Fla + Pyr) at 0.52 and BaA/(BaA + Chr) at 0.50 combined were also reflective of oil combustion (Galarnau, 2008), implicating emissions from food. On the other hand, there were a few values between 0.4 and 0.5 for Fla/(Fla + Pyr) and between 0.20 and 0.35 for BaA/(BaA + Chr), indications of liquid fossil fuel and crude oil combustion (Aceves and Grmlalt, 1993; Wang et al., 2016; Yunker et al., 2002). All these diagnostic results implicated that particle-bound PAHs at the 2-m site were predominantly derived from BBQ fumes, primarily generated from wood and charcoal combustion and food-charred emissions, as well as from petroleum combustion.

At the 10-m site, Fla/(Fla + Pyr) and Ant/(Ant + Phe) were in the ranges of 0.16–0.68 and 0.06–0.63, respectively (Table 2), indicating a combination of petrogenic and pyrogenic origins (Budzinski et al., 1997; Katsoyiannis et al., 2011; Yunker et al., 2002). The Fla/(Fla + Pyr) values in coarse particles ranged between 0.4 and 0.5, consistent with fuel combustion emissions, such as those from diesel- and

gasoline-powered vehicles. Again, there were a few Fla/(Fla + Pyr) values larger than 0.5, i.e., the 10-m site was also influenced by BBQ fumes. Nevertheless, particle-bound PAHs at the 10-m site were predominated by petrogenic sources, but slightly influenced by BBQ fumes due to wind direction and speed. It is noted that the average Ant/(Ant + Phe) value was slightly greater at the 2-m site (0.27) than at the 10-m site (0.23), similar to a previous finding that Ant/(Ant + Phe) decreased with increasing distance from a given emission source (Katsoyiannis and Breivik, 2014) and can be used to assess distance variability.

3.3. Personal air monitoring of PAHs

Personal samplers equipped with filters and absorbent materials (e.g., PUF, XAD-2, and XAD-4) have been used extensively for air monitoring, especially for personal air exposure assessment (Liu et al., 2014; Neri et al., 2016; Preuss et al., 2006; Sklorz et al., 2007). In the present study, personal samplers equipped with XAD-2 and XAD-4 resins were applied to estimate personal exposure to PAHs near the BBQ stoves. Only the low and moderate molecular-weight PAHs were detected in personal air samples (Table S1), but their concentrations (except for Nap) were much lower than those from MOUDI and PUF (Tables S1 and S2). A previous study employing a sampler equipped with filter and PUF/XAD-4/PUF sandwich also reported few detectable PAHs with molecular weights higher than Pyr (Xie et al., 2014). The mean concentration of Nap in personal air samples was 917 ng m^{-3} , compared to non-detected in PUF samples after correction by filed blank. This may have resulted from high break-through of Nap in PUF field samples (Hart et al., 1992), as well as strong sorption of atmospherically derived Nap in PUF blank. The mean values of Fla/(Fla + Pyr) and Ant/(Ant + Phe) in personal air samples were 0.64 and 0.10, respectively, also in agreement with pyrogenic and charcoal/wood combustion sources.

As our personal samplers were not equipped with particle filters, the samples collected contained both gaseous and particulate PAHs. However, the proportions of particulate PAHs (low to moderate molecular weights) collected with MOUDI were much smaller than those in the gaseous phase collected with PUF. Previous studies also indicated that 2–4 ring PAHs were predominant in the gaseous phase ($>97\%$) (Xie

Table 1

Geometric mean diameter (GMD; μm) and geometric standard deviations (GSD; μm) of particulate PAHs at 2 and 10 m sites away from BBQ stoves in Guangzhou.

	2 m		10 m	
	GMD	GSD	GMD	GSD
Acy	1.71	3.33	1.22	3.90
Ace	1.10	5.41	0.74	4.16
Flu	1.31	5.21	0.92	3.59
Phe	1.13	5.27	0.80	3.33
Ant	3.27	5.24	1.56	4.16
Fla	2.07	4.81	1.40	4.36
Pyr	2.19	5.11	1.06	5.12
BaA	1.43	4.19	1.34	4.89
Chr	1.08	3.47	0.70	4.79
B[b + k]F	0.86	4.78	0.60	1.72
BaP	0.43	2.42	0.75	1.00
IcdP	0.62	1.93	– ^a	–
DahA	–	–	–	–
BghiP	1.51	2.63	–	–

^a –: means data is not available.

Table 2
Mass ratios of PAH isomers in 11 particle size fraction (μm) at 2-m and 10-m sites away from BBQ stoves.

	>18	10–18	5.6–10	3.2–5.6	1.8–3.2	1.0–1.8	0.56–10	0.32–0.56	0.18–0.32	0.10–0.18	0.056–0.10	Total
2 m												
Fla/(Fla + Pyr)	0.47	0.49	0.51	0.53	0.56	0.54	0.52	0.50	0.53	0.40	0.56	0.51
Ant/(Ant + Phe)	0.44	0.43	0.36	0.55	0.30	0.13	0.10	0.14	0.19	0.15	0.17	0.27
BaA/(BaA + Chr)	0.59	0.51	0.48	0.57	0.51	0.35	0.36	0.32	0.51	0.51	0.31	0.42
10 m												
Fla/(Fla + Pyr)	0.53	0.27	0.33	0.68	0.18	0.42	0.53	0.37	0.36	0.16	0.30	0.44
Ant/(Ant + Phe)	0.49	0.51	0.42	0.29	0.63	0.19	0.19	0.37	0.06	0.09	0.26	0.23
BaA/(BaA + Chr)	– ^a	–	–	–	–	–	–	–	–	–	–	–

^a –: means data is not available.

et al., 2014; Zhao et al., 2011). Hence, concentrations of PAHs obtained with XAD resins were essentially representative of those in the gaseous phase, and could be used to estimate clothing-air partition coefficients with sufficient accuracy.

3.4. Clothing-air partitioning

The clothing-air partition coefficient ($K_{\text{area-0m}}$) obtained in XAD at 0-m was in the range of 2.0–290 m for PAHs with molecular weights lower than 228 (e.g., Chr) except for BaA (Table S3). The $\log K_{\text{area-0m}}$ values increased significantly ($p < 0.01$ and $r^2 = 0.82$) with increasing $\log K_{\text{OA}}$ (Fig. 4a). Saini et al. (2017, 2016) also obtained linear correlations between $\log K_{\text{area}}$ and $\log K_{\text{OA}}$ for phthalates and halogenated flame retardants in cotton clothes, as well as for polybrominated diphenyl ethers in cotton, polyester, and steel clothes. On the other hand, the clothing-air partition coefficients ($K_{\text{area-2m}}$) of PAHs obtained in PUF at the 2-m site ranged between 0.64 and 12 m for PAHs with molecular weights lower than 228 except for Nap (Table S3). There was no significant linear correlation ($p > 0.05$; Fig. 4b) between $\log K_{\text{area-2m}}$ and $\log K_{\text{OA}}$. As personal samplers were placed closer to cotton clothes than PUF, the clothing-air partition coefficients obtained with personal samplers were likely to be more reflective of reality and were used for further assessment below.

Morrison et al. (2018, 2015a, 2015b) estimated $\log K_{\text{area}}$ values for several organic chemicals in different fabrics. The $\log K_{\text{area}}$ values were in the range of 2.0–3.2 for methamphetamine in polyester and/or cotton clothes, 1.9–3.4 and <2.0–3.3 for PCB-28 and PCB-52, respectively, in fabric materials including 100% cotton, 100% polyester, and blends of cotton, polyester, viscose/rayon, and/or elastane, and 2.3–2.6 and 3.5–3.8 for diethyl phthalate and di-n-butyl phthalate, respectively, in cotton undershirt, outershirt, and jean. The area normalized clothing-air partition coefficients of PAHs obtained in the present study

(Table S3), especially for low-molecular weight PAHs, were generally lower than those presented above for other organic chemicals. The exceptions are Pyr and Chr, with $\log K_{\text{area}}$ values (2.1 and 2.5) comparable to those described above. Because the time for clothing exposure to PAHs was short, the clothes did not achieve equilibrium with atmospheric PAHs (Morrison et al., 2018; Morrison et al., 2015a; Saini et al., 2017), resulting in underestimated clothing-air partition coefficients of PAHs. Moreover, cotton clothes are consisted primarily of cellulose containing polar spots which are strong sorbents for polar species (Buchert et al., 2001; Morrison et al., 2015b). This is why less cotton clothes sorbed less amounts of PAHs compared to other polar compounds such as phthalate, nicotine, and methamphetamine (Morrison et al., 2015b; Saini et al., 2016). Finally, the hygroscopicity of cotton can reduce the sorption of lipophilic PAHs (Saini et al., 2017). Because clothing materials can strongly influence the absorption of different compounds (Morrison et al., 2018; Morrison et al., 2015b; Saini et al., 2016; Sherlach et al., 2011), appropriate fabric materials should be chosen to reduce PAHs exposure, especially for sensitive population groups such as toddlers.

4. Conclusions

Composition profiles and size distributions of PAHs were different between 2- and 10-m distances from the BBQ stoves. Particle-bound PAHs collected at both distances were mostly affiliated in fine particles. The $\log K_{\text{area}}$ values estimated from PAH concentrations in personal air samplers were significantly correlated with $\log K_{\text{OA}}$, and increased with increasing PAH molecular weight. The $\log K_{\text{area}}$ of lower molecular-weight PAHs in cotton clothes were lower than those of polar compounds, probably due to cellulose in cotton and lipophilicity of PAHs, as well as the non-equilibrium state of PAHs in clothes.

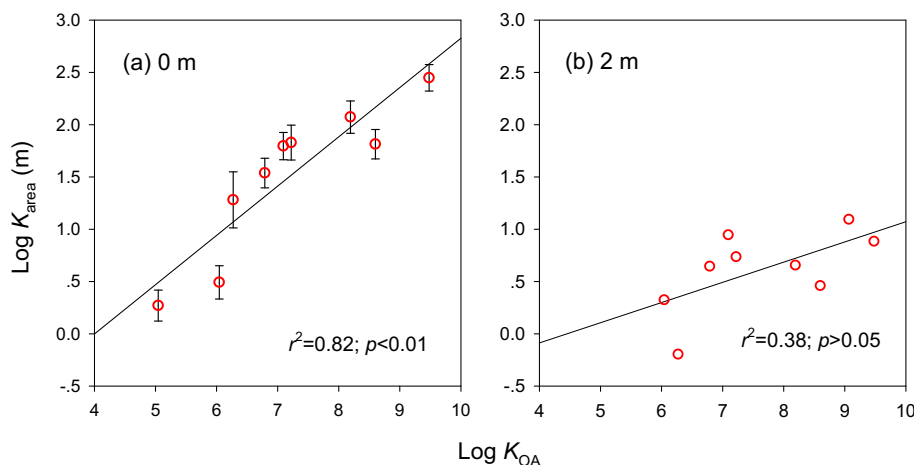


Fig. 4. Correlation between the logarithms of air-clothing and octanol-air partition coefficients for nine PAHs in (a) personal air samples (0 m from clothes) and (b) in PUF samples (2 m from clothes). $\log K_{\text{OA}}$ values of PAHs were obtained from EPI Suite.

Conflict of interest

The authors declare no competing financial interest.

Acknowledgments

The present study was financially supported by the National Natural Science Foundation of China (Nos. 41390240 and 21722701). We thank Shan-Yi Xie, Ting-Yu Li, Yuan-jie Hu, Yang Su, Jun-Feng Zhou, and Chun-Li Huang for field and laboratory support.

Appendix A. Supplementary data

Supplementary data to this article can be found online at <https://doi.org/10.1016/j.scitotenv.2018.05.220>.

References

- Aceves, M., Grimalt, J.O., 1993. Seasonally dependent size distributions of aliphatic and polynuclear hydrocarbons in urban aerosols from densely populated areas. *Environ. Sci. Technol.* 27, 2896–2908.
- Amouei Torkmahalleh, M., Gorjinezhad, S., Unluvecek, H.S., Hopke, P.K., 2017. Review of factors impacting emission/concentration of cooking generated particulate matter. *Sci. Total Environ.* 586, 1046–1056.
- Badyda, A.J., Widziewicz, K., Rogula-Kozłowska, W., Majewski, G., Jureczko, I., 2018. Inhalation exposure to PM-bound polycyclic aromatic hydrocarbons released from barbecue grills powered by gas, lump charcoal, and charcoal briquettes. *Adv. Exp. Med. Biol.* 1023, 11–27.
- Bi, X.H., Sheng, G.Y., Peng, P.A., Chen, Y.J., Zhang, Z.Q., Fu, J.M., 2003. Distribution of particulate- and vapor-phase n-alkanes and polycyclic aromatic hydrocarbons in urban atmosphere of Guangzhou, China. *Atmos. Environ.* 37, 289–298.
- Bi, X.H., Sheng, G.Y., Peng, P.A., Chen, Y.J., Fu, J.M., 2005. Size distribution of n-alkanes and polycyclic aromatic hydrocarbons (PAHs) in urban and rural atmospheres of Guangzhou, China. *Atmos. Environ.* 39, 477–487.
- Buchert, J., Pere, J., Johansson, L.S., Campbell, J.M., 2001. Analysis of the surface chemistry of linen and cotton fabrics. *Text. Res. J.* 71, 626–629.
- Budzinski, H., Jones, I., Bellocq, J., Picard, C., Garrigues, P., 1997. Evaluation of sediment contamination by polycyclic aromatic hydrocarbons in the Gironde estuary. *Mar. Chem.* 58, 85–97.
- Burkard, K., Nehls, I., Win, T., Endlicher, W., 2013. The carcinogenic risk and variability of particulate-bound polycyclic aromatic hydrocarbons with consideration of meteorological conditions. *Air Qual. Atmos. Health* 6, 27–38.
- Chen, J.W., Wang, S.L., Hsieh, D.P.H., Yang, H.H., Lee, H.L., 2012. Carcinogenic potencies of polycyclic aromatic hydrocarbons for back-door neighbors of restaurants with cooking emissions. *Sci. Total Environ.* 417–418, 68–75.
- Dvorská, A., Lammel, G., Klánová, J., 2011. Use of diagnostic ratios for studying source apportionment and reactivity of ambient polycyclic aromatic hydrocarbons over central Europe. *Atmos. Environ.* 45, 420–427.
- Farhadian, A., Jinap, S., Hanifah, H.N., Zaidul, I.S., 2011. Effects of meat preheating and wrapping on the levels of polycyclic aromatic hydrocarbons in charcoal-grilled meat. *Food Chem.* 124, 141–146.
- Galarnau, E., 2008. Source specificity and atmospheric processing of airborne PAHs: implications for source apportionment. *Atmos. Environ.* 42, 8139–8149.
- Gao, J., Jian, Y.T., Cao, C.S., Chen, L., Zhang, X., 2015. Indoor emission, dispersion and exposure of total particle-bound polycyclic aromatic hydrocarbons during cooking. *Atmos. Environ.* 120, 191–199.
- Hart, K.M., Isabelle, L.M., Pankow, J.F., 1992. High-volume air sampler for particle and gas sampling. 1. Design and gas sampling performance. *Environ. Sci. Technol.* 26, 1048–1052.
- Katsoyiannis, A., Breivik, K., 2014. Model-based evaluation of the use of polycyclic aromatic hydrocarbons molecular diagnostic ratios as a source identification tool. *Environ. Pollut.* 184, 488–494.
- Katsoyiannis, A., Sweetman, A.J., Jones, K.C., 2011. PAH molecular diagnostic ratios applied to atmospheric sources: a critical evaluation using two decades of source inventory and air concentration data from the UK. *Environ. Sci. Technol.* 45, 8897–8906.
- Kavouras, I.G., Stephanou, E.G., 2002. Particle size distribution of organic primary and secondary aerosol constituents in urban, background marine, and forest atmosphere. *J. Geophys. Res.* 107, 1–12.
- Lee, W.J., Wang, Y.F., Lin, T.C., Chen, Y.Y., Lin, W.C., Ku, C.C., et al., 1995. PAH characteristics in the ambient air of traffic-source. *Sci. Total Environ.* 159, 185–200.
- Li, Z., Mulholland, J.A., Romanoff, L.C., Pittman, E.N., Trinidad, D.A., Lewin, M.D., et al., 2010. Assessment of non-occupational exposure to polycyclic aromatic hydrocarbons through personal air sampling and urinary biomonitoring. *J. Environ. Monit.* 12, 1110–1118.
- Liu, LiY, Kukucka, P., Venier, M., Salamova, A., Klanova, J., Hites, R.A., 2014. Differences in spatiotemporal variations of atmospheric PAH levels between North America and Europe: data from two air monitoring projects. *Environ. Int.* 64, 48–55.
- Luo, P., Bao, L.J., Li, S.M., Zeng, E.Y., 2015. Size-dependent distribution and inhalation cancer risk of particle-bound polycyclic aromatic hydrocarbons at a typical e-waste recycling and an urban site. *Environ. Pollut.* 200, 10–15.
- Mode, d. Types of fuel <http://www.mode.co.uk/types-of-fuel.shtml> (December 26, 2017).
- Morrison, G.C., Li, H.W., Mishra, S., Buechlein, M., 2015a. Airborne phthalate partitioning to cotton clothing. *Atmos. Environ.* 115, 149–152.
- Morrison, G.C., Shakila, N.V., Parker, K., 2015b. Accumulation of gas-phase methamphetamine on clothing, toy fabrics, and skin oil. *Indoor Air* 25, 405–414.
- Morrison, G.C., Weschler, C.J., Beko, G., Koch, H.M., Salthammer, T., Schripp, T., et al., 2015c. Role of clothing in both accelerating and impeding dermal absorption of airborne SVOCs. *J. Expo. Sci. Environ. Epidemiol.* 26, 113–118.
- Morrison, G.C., Andersen, H.V., Gunnarsen, L., Varol, D., Uhde, E., Kolarik, B., 2018. Partitioning of PCBs from air to clothing materials in a Danish apartment. *Indoor Air* 28, 188–197.
- Neri, F., Foderi, C., Laschi, A., Fabiano, F., Cambi, M., Sciarra, G., et al., 2016. Determining exhaust fumes exposure in chainsaw operations. *Environ. Pollut.* 218, 1162–1169.
- Odabasi, M., Cetin, B., Bayram, A., 2015. Persistent organic pollutants (POPs) on fine and coarse atmospheric particles measured at two (urban and industrial) sites. *Aerosol Air Qual. Res.* 15, 1894–1905.
- Oz, F., Yuzer, M.O., 2016. The effects of cooking on wire and stone barbecue at different cooking levels on the formation of heterocyclic aromatic amines and polycyclic aromatic hydrocarbons in beef steak. *Food Chem.* 203, 59–66.
- Preuss, R., Roßbach, B., Wilhelm, M., Bruning, T., Angerer, J., 2006. External and internal exposure to polycyclic aromatic hydrocarbons (PAH) among workers in the production of fire-proof materials - proposal of a biological monitoring guidance value. *Int. J. Hyg. Environ. Health* 209, 575–580.
- Rey-Salgueiro, L., Martínez-Carballo, E., García-Falcón, M.S., Simal-Gándara, J., 2008. Effects of a chemical company fire on the occurrence of polycyclic aromatic hydrocarbons in plant foods. *Food Chem.* 108, 347–353.
- Saini, A., Rauer, C., Simpson, M.J., Harrad, S., Diamond, M.L., 2016. Characterizing the sorption of polybrominated diphenyl ethers (PBDEs) to cotton and polyester fabrics under controlled conditions. *Sci. Total Environ.* 563–564, 99–107.
- Saini, A., Okeme, J.O., Mark Parnis, J., McQueen, R.H., Diamond, M.L., 2017. From air to clothing: characterizing the accumulation of semi-volatile organic compounds to fabrics in indoor environments. *Indoor Air* 27, 631–641.
- Saito, E., Tanaka, N., Miyazaki, A., Tsuzaki, M., 2014. Concentration and particle size distribution of polycyclic aromatic hydrocarbons formed by thermal cooking. *Food Chem.* 153, 285–291.
- Schnelle-Kreis, J., Jansch, T., Wolf, K., Gebefugi, I., Kettrup, A., 1999. The effect of wind direction on the observed size distribution of particle adsorbed polycyclic aromatic hydrocarbons on an inner city sampling site. *J. Environ. Monit.* 1, 357–360.
- Sherlach, K.S., Gorka, A.P., Dantzer, A., Roepe, P.D., 2011. Quantification of perchloroethylene residues in dry-cleaned fabrics. *Environ. Toxicol. Chem.* 30, 2481–2487.
- Sioutas, C., Delfino, R.J., Singh, M., 2005. Exposure assessment for atmospheric ultrafine particles (UFPs) and implications in epidemiologic research. *Environ. Health Perspect.* 113, 947–955.
- Sklorz, M., Schnelle-Kreis, J., Liu, Y.B., Orasche, J., Zimmermann, R., 2007. Daytime resolved analysis of polycyclic aromatic hydrocarbons in urban aerosol samples - impact of sources and meteorological conditions. *Chemosphere* 67, 934–943.
- Tsapakis, M., Stephanou, E.G., 2005. Occurrence of gaseous and particulate polycyclic aromatic hydrocarbons in the urban atmosphere: study of sources and ambient temperature effect on the gas/particle concentration and distribution. *Environ. Pollut.* 133, 147–156.
- USEPA Regional Removal Management Levels (RMLs) Frequently Asked Questions (January 3, 2017).
- Van Vaeck, L., Van Cauwenbergh, K.A., 1985. Characteristic parameters of particle size distributions of primary organic constituents of ambient aerosols. *Environ. Sci. Technol.* 19, 707–716.
- Wang, G., Cheng, S.Y., Wei, W., Wang, X.Q., Yao, S., 2015. Chemical characteristics of fine particles emitted from different Chinese cooking styles. *Aerosol Air Qual. Res.* 15, 2357–2366.
- Wang, Q.Y., Kobayashi, K., Lu, S.L., Nakajima, D., Wang, W.Q., Zhang, W.C., et al., 2016. Studies on size distribution and health risk of 37 species of polycyclic aromatic hydrocarbons associated with fine particulate matter collected in the atmosphere of a sub-urban area of Shanghai city, China. *Environ. Pollut.* 214, 149–160.
- Wang, L.A., Xiang, Z.Y., Stevanovic, S., Ristovski, Z., Salimi, F., Gao, J., et al., 2017. Role of Chinese cooking emissions on ambient air quality and human health. *Sci. Total Environ.* 589, 173–181.
- Wu, C.C., Bao, L.J., Guo, Y., Li, S.M., Zeng, E.Y., 2015. Barbecue fumes: an overlooked source of health hazards in outdoor settings? *Environ. Sci. Technol.* 49, 10607–10615.
- Xie, M.J., Hannigan, M.P., Barsanti, K.C., 2014. Gas/particle partitioning of n-alkanes, PAHs and oxygenated PAHs in urban Denver. *Atmos. Environ.* 95, 355–362.
- Yao, Z.L., Li, J., Wu, B.B., Hao, X.W., Yin, Y., Jiang, X., 2015. Characteristics of PAHs from deep-frying and frying cooking fumes. *Environ. Sci. Pollut. Res.* 22, 16110–16120.
- Yunker, M.B., Macdonald, R.W., Vingarzan, R., Mitchell, R.H., Goyette, D., Sylvestre, S., 2002. PAHs in the Fraser River basin: a critical appraisal of PAH ratios as indicators of PAH source and composition. *Org. Geochem.* 33, 489–515.
- Zhao, P., Yu, K.P., Lin, C.C., 2011. Risk assessment of inhalation exposure to polycyclic aromatic hydrocarbons in Taiwanese workers at night markets. *Int. Arch. Occup. Environ. Health* 84, 231–237.